Heterolytic Adsorption of H_2 on ZnO($10\bar{1}0$) Surface: An ab initio SPC Cluster Model Study

Xin Lü, Xin Xu,* Nanqin Wang, and Qianer Zhang

State Key Laboratory for Physical Chemistry of Solid Surfaces; Department of Chemistry, Institute for Physical Chemistry, Xiamen University, Xiamen, 361005, People's Republic of China

Masahiro Ehara and Hiroshi Nakatsuji*

Department of Synthetic Chemistry and Biological Chemistry, Graduate School of Engineering, Kyoto University, Kyoto 606-01, Japan

Received: February 26, 1998; In Final Form: December 7, 1998

Heterolytic adsorption of H_2 on ZnO($10\bar{1}0$) surface has been investigated by means of ab initio embedded cluster method. The embedding point charges are spherically expanded, while the values of the spherical charges are determined to be self-consistent with those of the atoms in the cluster. Several possible adsorption sites have been considered with Zn_5O_5 and Zn_4O_4, which are the stoichiometric clusters having the least amount of dangling bonds in the given size. The effect of the shape of the embedding spherical charge array and the influence of the surface reconstruction on the calculated adsorption properties have been investigated. The calculation results show that the heterolytic adsorption of H_2 on ZnO($10\bar{1}0$) surface is site-dependent, taking place only on those Zn−O ion-pairs with low coordination numbers, such as $Zn_{2c}-O_{3c}$, $Zn_{3c}-O_{2c}$, and $Zn_{2c}-O_{2c}$, rather than on the perfect ion pair, $Zn_{3c}-O_{3c}$. The calculated adsorption heats, as well as vibrational frequencies of the Zn−H and O−H bonds, are in reasonable agreement with the experimental values.

1. Introduction

The adsorption of H_2 on ZnO has been of interest for several decades due to its close relationship with some industrially important processes, e.g., hydrogenation of olefins, methanol synthesis from syngas, and water-gas shift reaction. Plenty of experimental evidences showed that ZnO works to provide sites for the chemisorption of H_2.[1−5] The so-called type I adspecies, which are IR-active, were believed to derive from heterolytic chemisorption of H_2,[2−10] i.e.,

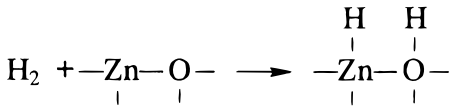

and have been shown to be the main resource of hydrogen for methanol synthesis and hydrogenation of ethylene.[3,4] On the other hand, the TPD experiment revealed that those type I adspecies cover only about 5−10% of the surface sites on the ZnO powder catalysts[6,7] with the desorption heat in the range of 28−31 kcal/mol.[7,8] Since the most stable surfaces of ZnO solid are those nonpolar ($10\bar{1}0$) and ($11\bar{2}0$) surfaces, in which Zn and O surface ions are 3-fold coordinated, the observation thereby implies that no regular $Zn_{3C}-O_{3C}$ ion-pairs of these surfaces should be responsible for the dissociative chemisorption of H_2, and the most possibly active sites should be those defective surface sites, such as $Zn_{2c}-O_{3c}$, $Zn_{3c}-O_{2c}$, and $Zn_{2c}-O_{2c}$, presenting at the edge and corner sites of ZnO surfaces. In other words, heterolytic adsorption of H_2 on ZnO should be site-dependent.

Theoretically, some relevant papers have been published. A bare cluster of $Zn_{14}O_{14}$ has been employed to model the ZnO-($10\bar{1}0$) surface by Anderson and Nichols, and the adsorptions of H•, H^+, and H^- have been investigated with the semiempirical ASED-MO (atom superposition and electron delocalization molecular orbital) method.[11] They found that heterolytic adsorption of H_2 leads to strong O−H and Zn−H bonds; homolytic adsorption, however, leads to two weak Zn−H bonds. Nakatsuji and Fukunishi,[12] by embedding a ZnO molecule into the nearest 32 point charges in values of ±0.5au to mimic the $Zn_{3c}-O_{3c}$ ion-pair on the ideal ZnO($10\bar{1}0$) surface, exploited the reaction path of H_2 dissociation by using HF (Hartree−Fock) method and SAC/SAC-CI (symmetry-adapted cluster configuration interaction) method. The dissociation of H_2 on ZnO has been described as an electron donation from the $2p\pi$ orbital of oxygen to the antibonding σ_u MO of H_2 and a back-donation of the bonding σ_g MO of H_2 to the LUMO (lowest unoccupied molecular orbital) of ZnO; the polarity of ZnO assists these frontier orbital interactions. The calculated vibrational frequencies ν_e(O−H) and ν_e(Zn−H) are 4090 and 1730 cm^{-1}, respectively, in accordance with the experimental values of 3510 and 1710 cm^{-1}.[9] The predicted heat of reaction (73.5 kcal/mol) is overestimated with respect to the experimental estimation of Waugh et al. (28−31 kcal/mol).[7,8] Recently, Rohl et al. performed atomistic modeling of reconstruction and relaxation of the nonpolar ($10\bar{1}0$), ($11\bar{2}0$) surfaces and the polar (0001) surface of ZnO, as well as ab initio embedded cluster calculations of heterolytic chemisorption of H_2 on these surfaces.[13] Very little differential effects of relaxation on the vertical

* Corresponding authors. E-mail: xinxu@xmu.edu.cn; hiroshi@sbchem.kyoto-u.ac.jp. Fax: +86-592-2183047; +81-75-753−5910.

10.1021/jp981309w CCC: $18.00
Published on Web 03/24/1999

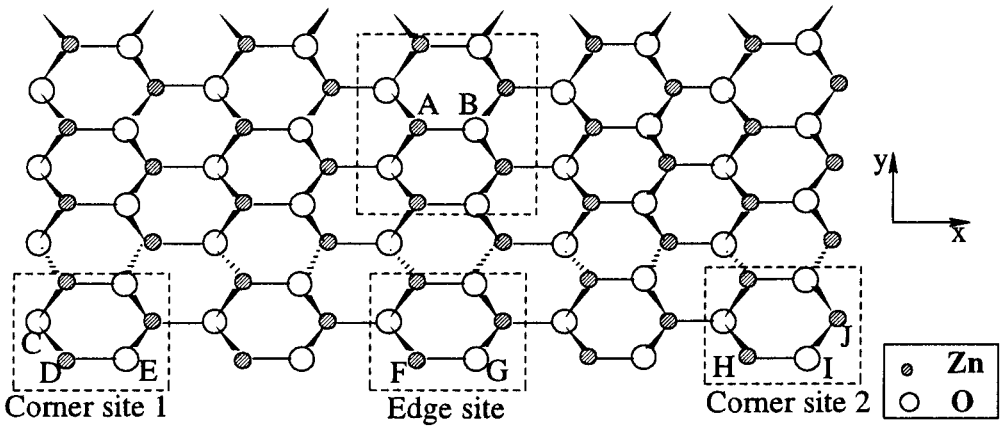

Figure 1. Structure of the ZnO wurtzite crystal lattice (Top view of the ZnO($10\bar{1}0$) surface. The active sites for H_2 chemisorption are labeled alphabetically.).

separation of the cations and the anions were found for the two nonpolar surfaces and the two nonpolar surfaces were found to be unreactive toward H_2 dissociation. The defective sites at the reconstructed (0001) surface were shown to be able to cause exothermic reaction of H_2 dissociation. The determining factor for the exothermicity was correlated with the coordination of the anion.[13] The HF adsorption heats ranged from 6.0 to 103.0 kcal/mol; while the MCPF (modified coupled pair functional) ones from 6.0 to 27 kcal/mol. The HF vibrational frequencies for the O−H bond (range: 2339−3686 cm^{-1}) were qualitatively in agreement with experimental values, while those for the Zn−H vibrations (range: 713−1554 cm^{-1}) were lower than the experimental values. More recently, Martins et al. used an ab initio HF method with $(ZnO)_n$ (n = 6, 8) clusters as well as MNDO, AM1, and PM3 semiempirical methods with large clusters of $(ZnO)_n$ (n = 22, 44, 60) to study the molecular adsorption and dissociation of H_2 on ZnO surfaces.[14,15] They predicted that the preferential site for heterolytic H_2 dissociation is the oxygen which has a coordination number of two, and the H_2 dissociation shows a large stabilization energy for the most stable adsorption site which is the lowest coordination site. Geometry optimizations have been performed, while no detailed vibrational frequencies of Zn−H and O−H have been presented.[14,15] The reaction heats of H_2 dissociation over various sites of ZnO surfaces were greatly overestimated.[14,15]

In the cluster modeling of metal oxides, one has to answer two questions: (i) how to cut out a cluster; and (ii) how to suitably account for the cluster−lattice interaction. For the first question, we have proposed three principles, namely, a neutrality principle, a stoichiometrical principle, and a coordination principle,[16,17] according to which a neutral, stoichiometrical cut-out cluster with the minimal amount of dangling bonds is preferred.[17,18] Our ab initio studies for ZnO solid[17] and CO/ZnO chemisorption system[18] have shown a good correlation between the topologic parameters N_d (the total amount of dangling bonds of a cutout cluster) and β (the average dangling bonds on each in-cluster atom) with the stability of clusters, which provides an efficient way to set up a better cluster model of a given size. For the second question, if the surrounding of a cut-out cluster is approximately simulated by a point charge cluster (PCC), the cluster−lattice interaction could be described by means of the Madelung potential.[19,20] One of the basic questions which confronts us in this procedure is in what values the embedding point charges should be for a given metal oxide. In the sake of simplicity, nominal charges are always used. However, it is clear that certain requirements for the consistence between the charges derived from the embedded cluster and those in the PCC should be reached, since they are all representatives of the equivalent atoms of an infinite crystal. Another weakness of using point charges to replace the real atoms lies in that the Pauli repulsion is ignored. For this, the so-called AIMP (total-ion ab initio model potential) formalism[13,21] provides a remedy. In a previous paper regarding CO/NiO(100) chemisorption system, we proposed a charge-consistent embedded cluster model,[22] where the point charges for embedding were set equal to the Mulliken charges on the respective in-cluster atoms. Some stimulating results were obtained.[22] Recently, we have proposed a cluster model called SPC,[23,24] where PC, as usual, stands for the *point charge* embedding technique; S has several meanings such as a *stoichiometric* cutout cluster with the least dangling bonds embedded in a *symmetric* PCC, and a *spherically* expanded point charge surrounding with charges being *self-consistently* determined.[23,24] We have studied several representative chemisorption systems, e.g., CO/MgO, O/MgO, CO/ZnO, O/ZnO, H_2/ZnO, H_2/TiO_2, etc., with the SPC cluster model method and have investigated the effects of size and symmetry of PCC, size dependence of cluster model, basis sets, electron correlation on the theoretical description of chemisorptive bonding. In this paper, the results on the heterolytic chemisorption of H_2 on ZnO ($10\bar{1}0$) surface are reported. Several possible adsorption sites, i.e., the regular site, the edge sites, and the corner sites, on the ($10\bar{1}0$) surface have been considered. The effect of the shape of PCC and the influence of the surface reconstruction on the calculated adsorption properties have been investigated.

2. Computational Details

Zinc oxide has the wurtzite structure.[25] The ideal ($10\bar{1}0$) surface, which is the most stable surface of ZnO solid, is shown in Figure 1. On the perfect ZnO($10\bar{1}0$) surface, only the Zn_{3c}−O_{3c} ion pairs are available, while at the edge and the corner of the ZnO($10\bar{1}0$) surface, the ion pairs having low coordination number are present. Therefore, we have several types of Zn−O ion pairs to be considered, i.e., Zn_{3c}−O_{3c} at the regular site, Zn_{2C}−O_{2C} at the edge site, and Zn_{3C}−O_{2C}, Zn_{2C}−O_{3C}, and Zn_{2C}−O_{2C} at the corner sites. To mimic these sites, two atomic clusters, i.e., Zn_5O_5 and Zn_4O_4 (Figure 2), are used and are located at the corresponding sites (cf. Figure 1) of a microcrystal consisting of a six-layer model of a total of 630 lattice atoms, within which the rest of the atoms are replaced by spherical charges. The Zn and O atoms of the active ion-pairs concerned are all labeled alphabetically in Figure 1. This gives six embedded cluster models, i.e., Zn_5O_5 for the Zn_{3C}−O_{3C} (A−

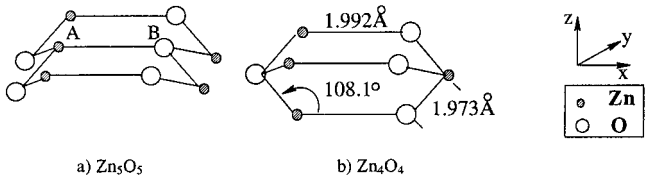

Figure 2. Zn_5O_5 and Zn_4O_4 clusters as models of the ZnO(10$\bar{1}$0) surface.

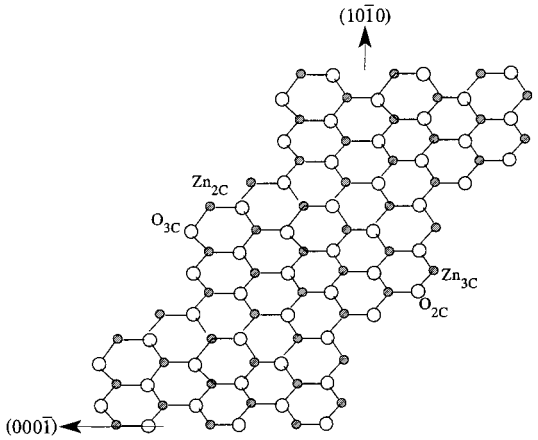

Figure 3. Reconstructed O-(000$\bar{1}$) and Zn−(0001) polar surfaces derived from LEED experiments (side view).

B) ion pair on the ideal surface; Zn_4O_4 for the $Zn_{2C}-O_{3C}$ (D−C) or the $Zn_{2C}-O_{2C}$ (D−E) on the corner site 1; the $Zn_{2C}-O_{2C}$ (F−G) at the edge site; and the $Zn_{2C}-O_{2C}$ (H−I) or the $Zn_{3C}-O_{2C}$(J−I) on the corner site 2 (cf. Figures 1 and 2). In these models, surface reconstruction and relaxation have not been taken into account.

The effects of surface reconstruction and relaxation are comparably smaller for the nonpolar (10$\bar{1}$0) surface than for the polar (0001) and (000$\bar{1}$) surfaces. However, $Zn_{2C}-O_{3C}$ or $Zn_{3C}-O_{2C}$ pairs at the corner can also be viewed as sites of (0001) and (000$\bar{1}$) surfaces. The neglecting of the surface reconstruction and relaxation should lead to overestimation of the reactivity of these sites. Unfortunately, it is impossible to optimize the surface structures within the point charge model, since no repulsive force between a positive charge and a negative charge is introduced. In fact, no satisfactory theoretical treatment of surface reconstruction and relaxation seems available.[13] In the present work, we adopt the experimental LEED pattern[26−31] (see Figure 3). A preliminary comparison between the adsorption properties of the ideal sites and those of the reconstructed sites is of value.

The spherical expansion of point charge Q_p is processed as follows:[23,24]

$$q_p(r) = Q_p(\varphi_s(r))^2 \tag{2.1}$$

$$Q_p = \int q_p(r)\mathrm{d}\tau \tag{2.2}$$

where

$$\varphi_s(r) = \left(\frac{2\alpha}{\pi}\right)^{3/4} \mathrm{e}^{-\alpha r^2} \tag{2.3}$$

is the spherical Gauss function; and $q_p(r)$ is the charge density.

From eqs 2.1−2.3 it can be easily deduced that the orbital exponent α is inversely proportional to the square of the orbital radius $\langle r\rangle$. Substituting the orbital radius $\langle r\rangle$ with the ion radius

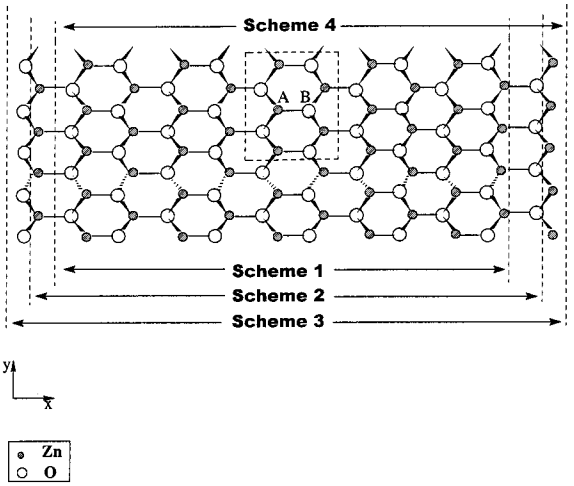

Figure 4. Embedding schemes (1−4) for the modeling of $Zn_{3C}-O_{3C}$ (A−B) pair site on ZnO (10$\bar{1}$0) surface. (Top-view of the ZnO (10$\bar{1}$0) surface).

$\langle R\rangle$, we found that the $\langle R\rangle$ and the exponent α obey the relation of

$$\alpha = \frac{3}{2\langle R\rangle^2} \tag{2.4}$$

For wurtzite ZnO, we have $\langle R_{Zn^{2+}}\rangle = 0.74$ Å, $\alpha_{Zn} = 0.7670$ Å^{-2}, and $\langle R_{O^{2-}}\rangle = 1.26$ Å, $\alpha_O = 0.2646$ Å^{-2}.

A series of $(ZnO)_n$ ($n = 3-13$) SPC cluster models have been employed to simulate ZnO bulk solid.[18] The embedding spherical charges of cations and anions were self-consistently determined to be around the values of ±1.0 au. Therefore, the values of ±1.0 au are used for the embedding spherical charges in the present work. The values of Q_ps depend, to some extent, on the basis sets employed and the correlation treatment. In practice, we found that Q_ps are quite stable, if $(ZnO)_n$ clusters are moderately large(say $n \geq 4$).

The influence of the shape of PCC on the calculated adsorption properties has been examined with different embedding schemes (see Figure 4).

The basis set for the Zn atom at the active site is the Ar ECP+(3s2p5d)/[2s2p2d] basis set of Hay and Wadt,[32] while that for the active O atom is Dunning's [4s2p] basis set[33] plus a diffuse sp function (exponent: 0.059) and a polarization d function (exponent: 0.30). The basis set for H atoms is the 21G plus a diffuse sp function (exponent: 0.036). For the other in-cluster atoms, smaller basis sets are employed. They are the Ar ECP+(3s2p5d)/[1s1p1d] basis set of Hay and Wadt[32] for Zn atoms and the CEP-31G[34] for O atoms.

The adsorption geometries of H_2 are optimized by using the HF method in the cases of the bared clusters with all the substrate atoms being fixed. In the embedded cases, the bond angles of the adsorption bonds are fixed in the optimized geometries of the bare clusters, while the equilibrium bond distances (R_{ZnH} and R_{OH}) and vibrational frequencies (ν_e(Zn−H) and ν_e(O−H)) are determined by a fourth-degree polynomial fit to five points around the minimum of the corresponding potential energy curves. The effect of correlation is taken into account with the second-order Moller−Plesset (MP2) method. We also consider the smallest cluster model, ZnO unit, for which the geometries from the early work are adopted.[12]

Test calculations with the present methodology on OH^{δ} and ZnH^{δ} dimers are listed in Table 1. The results are in reasonably good agreement with the experimental values. All calculations

TABLE 1: Test Calculations on OH^- and ZnH^+ Dimers

	D_e(eV)[b]			R_e(Å)			ν_e(cm^{-1})		
	HF	MP2	exptl[c]	HF	MP2	exptl[c]	HF	MP2	exptl[c]
OH	2.61	3.92	4.39	0.974	0.990	0.97	3892	3678	3738
OH^-	2.73	5.62	5.47	0.965	0.984	0.97	3902	3712	3700
ZnH	0.67	0.68	0.85	1.661	1.650	1.59	1511	1527	1608
ZnH^+	6.97	6.93	7.09[d]	1.562	1.565	1.51	1912	1854	1916

[a] Calculated dissociation energies, D_e, optimized bond lengths, and vibrational frequencies using methodology employed to study heterolytic adsorption of H_2 on ZnO($10\bar{1}0$) surface. [b] These refer to the binding of H^+, H, and H^- to O and Zn. [c] Experimental results in parentheses are from Huber, K. P.; Herzberg, G. *Molecular Structure IV, Constants for Diatomic Molecules*; van Nostrand: New York, 1979. [d] Calculation results with 6-311++G(3df,3pd) basis set for Zn.

are performed with the Gaussian 94 package[35] on SGI Power Indigo^2 workstations.

3. Electronic Properties of the Bared Clusters and the Embedded Clusters

Table 2 presents the results of HF calculations for the bared clusters and the embedded clusters (cf. Figures 1 and 2). The energy levels of HOMO (highest occupied molecular orbitals) and LUMO (lowest unoccupied molecular orbitals) and the energy gaps, ΔG, between HOMO and LUMO are included, together with the average Mulliken charges of the in-cluster Zn and O ions.

The Mulliken charges of Zn and O atoms are predicted to be about ± 0.5 au for the bared ZnO dimer. For the embedded ZnO dimer the charges of Zn and O atoms are self-consistently determined to be ± 1.36 au. The dipole moment of the embedded ZnO dimer being 3−4 times that of the bared ZnO dimer provides evidence that embedding enhances the ionicity of the ZnO dimer. The energy gap between HOMO and LUMO of the ZnO dimer is also enlarged considerably upon embedding, implying an embedding-induced stabilization of the ZnO dimer. For the Zn_5O_5 cluster, the situation is rather mild. The Mulliken charges of Zn and O atoms are about ± 0.9 au for the bare cluster; for the embedded case, the averaged values are ± 1.03 au, similar to the embedding spherical charges derived from the bulk solid. The energy gap between its HOMO and LUMO also increases upon embedding, but to a less degree. As shown in Table 2, the calculated electronic properties of the ZnO dimer are of greater dependence on embedding than those of the larger clusters such as Zn_5O_5.

For the Zn_4O_4 models of the various defect sites, the calculated properties differ considerably. It is reasonable to assume that ions at differently coordinated and exposed sites at the surface should have a variable ionicity and different amounts of covalent character in Zn−O interactions. As shown in Table 2, embedding the Zn_4O_4 cluster at corner site 1 results in a significant increase of the HOMO energy of the cluster. As the HOMO is mainly O_{3c}(C) 2p-derived, the increase of this MO energy level implies the enhancement of the nucleophilicity of the O_{3c}(C) anion site. On the other hand, embedding the Zn_4O_4 cluster at corner site 2 largely stabilizes its HOMO and LUMO. Detailed population analysis reveals that the LUMO of this cluster is mainly Zn_{3C}(J) 4sp-like. The significant stabilization of the LUMO implies a considerable enhancement of the electrophilicity of the Zn_{3C}(J) site. It is believed that either the enhancement of nucleophilicity or enhancement of the electrophilicity of the active sites will increase the reactivity of the heterolytic dissociation of H_2. For Zn_4O_4 embedded at the edge site, embedding enlarges the energy gap between its HOMO and LUMO with respect to the bared cluster, which may imply a decrease of its reactivity to H_2.

4. Heterolytic Adsorption of H_2 on the Zn−O Ion Pairs of Ideal ($10\bar{1}0$) Surface

A. H_2 Adsorption on the Bared Clusters. The optimized geometries of heterolytically adsorbed hydrogen on the bared clusters are given in Table 3, as well as the corresponding heats of adsorption.

For the H_2 adsorption on the $Zn_{3C}-O_{3C}$(A−B) perfect ion pair, the calculated adsorption heat of H_2 on the bared ZnO dimer is rather exothermic with adsorption heat of 94.3 kcal/mol at the SCF level and of 87.5 kcal/mol at the MP2 level, in agreement with the previous calculations performed by SAC/SAC-CI.[12] For the bared Zn_5O_5 cluster, however, the H_2 adsorption on the perfect ion pair is predicted to be endothermic both at the SCF level and at the MP2 level. This theoretical prediction agrees qualitatively with the recent theoretical prediction of Rohl et al.[13] and the experimental deduction.[7,8] It seems that the ZnO dimer is too small to model the ZnO surface, and that a larger cluster, which includes the atoms neighboring with the active sites, is needed in order to obtain a qualitative description for H_2 adsorption on the $Zn_{3C}-O_{3C}$ perfect ion pair of the ideal ($10\bar{1}0$) surface.

For the defective ion pairs of $Zn_{2C}-O_{3C}$(D−C), $Zn_{3C}-O_{2C}$-(J−I), and $Zn_{2C}-O_{2C}$(F−G) with the bared Zn_4O_4 cluster models, the calculation demonstrates that the former two defect sites show weaker reactivity to H_2 with adsorption heats of less than 10.0 kcal/mol, whereas the $Zn_{2C}-O_{2C}$(F−G) ion pair is highly reactive to H_2 with a reaction heat of more than 65 kcal/mol. Their reactivity to dissociate H_2 follows the order of $Zn_{2C}-O_{2C} \gg Zn_{3C}-O_{2C} \cong Zn_{2C}-O_{3C}$, showing that the activity of the Zn−O ion pairs to H_2 chemisorption is dependent on the coordination numbers of Zn and O atoms. A similar trend was encountered by Sawabe et al.[36] and Kobayashi et al.[37] in their ab initio studies of H_2 adsorption on MgO. Coincidentally, the optimized H−X (X = Zn, O) bond lengths also show dependence on the coordination numbers of the active ions, i.e., the lower the coordination number the X ion possesses, the shorter the H−X bond length is. However, the results from the bared cluster model calculations could only be regarded as qualitative since the effect of the crystal potential is ignored. The calculated adsorption heats with the bare Zn_4O_4 cluster models are either too low (3.0−8.0 kcal/mol) or too high (65.0−87.2 kcal/mol) as compared with the experimental value (∼30.0 kcal/mol[7,8]).

B. H_2 Chemisorption on the Embedded Clusters. The calculated heats of H_2 chemisorption on the active sites of the embedded clusters are also given in Table 3. By comparing them with those of the nonembedded cases, the effect of embedding is obvious. For the ZnO dimer, embedding greatly decreases its reactivity in a value of more than 60 kcal/mol, both at the level of HF and at the level of MP2. However, embedding still fails to lead the minimal cluster model of the ZnO dimer to predict the reaction endothermic.

For the modeling of the $Zn_{3C}-O_{3C}$(A−B) perfect ion pairs with Zn_5O_5, the calculated properties seem to be less dependent on the embedding procedure. The chemisorption is predicted to be thermodynamically unfavorable, in accordance with the experimental observations[6] and that predicted with bare cluster model in the previous section. The embedding-induced change of the reactivity of the active ion pair, which is rather significant for the ZnO dimer, is mild for Zn_5O_5. It implies that the smaller the cut-out cluster is, the more rigorous the embedding technique that is required.

TABLE 2: Calculated Properties of Surface Clusters

cluster model/active sites		q_{spc} (au)	HOMO (eV)	LUMO (eV)	ΔG (eV)	Q_{Zn} (au)	Q_O (au)
ZnO							
$Zn_{3c}-O_{3c}$(A−B)	bared		−9.117	−0.509	8.608	+0.46	−0.46
	embedded	±1.36	−9.505	+1.456	10.961	+1.36	−1.36
Zn_5O_5							
$Zn_{3c}-O_{3c}$(A−B)	bared		−8.845	−1.222	7.623	+0.93	−0.93
	embedded	±1.00	−9.387	−0.888	8.499	+1.03	−1.03
Zn_4O_4							
$Zn_{2c}-O_{3c}$(D−C)	bared		−8.847	−1.192	7.655	+0.93	−0.93
	corner 1	±1.00	−3.832	+4.000	7.832	+1.09	−1.09
$Zn_{3c}-O_{2c}$(J−I)	bared		−8.934	−1.178	7.756	+0.99	−0.99
	corner 2	±1.00	−13.699	−5.891	7.808	+1.18	−1.18
$Zn_{2c}-O_{2c}$(F−G)	bared		−8.874	−1.032	7.842	+1.01	−1.01
	edge	±1.00	−9.136	+0.246	9.382	+1.24	−1.24
$Zn_{2c}-O_{2c}$(D−E)	corner 1	±1.00	−3.946	+3.419	7.365	+1.22	−1.22
$Zn_{2c}-O_{2c}$(H−I)	corner 2	±1.00	−13.539	−5.002	8.537	+1.21	−1.21

TABLE 3: Calculated Geometries, Heats,[a] and Frequencies for H_2/ZnO Chemisorption System

							ν_e(cm^{-1})	
cluster model[b]/active sites		R_{OH} (Å)	∠HOM (°)	R_{MH} (Å)	∠HMO (°)	ΔE (kcal/mol)	Zn−H	O−H
ZnO								
$Zn_{3C}-O_{3C}$(A−B)	bared	0.967	111.0	1.713	146.0	94.3		
						87.5[e]		
	embedded					27.0	1807	4078
						11.9[e]		
Zn_5O_5								
$Zn_{3C}-O_{3C}$(A−B)	bared	0.965	95.5	1.774	81.2	−23.5		
						−27.5[e]		
	embedded	0.962		1.778		−22.9	1262	3864
		0.985[e]		1.735[e]		−23.2[e]	1341[e]	3531[e]
Zn_4O_4								
$Zn_{2C}-O_{3C}$(D−C)	bared	0.961	93.8	1.642	93.5	8.0		
						3.0[e]		
	corner 1	0.960		1.649		48.3	1595	3986
		0.980[e]		1.627[e]		38.5[e]	1652[e]	3705[e]
	reconst. step	0.962		1.614		21.0	1753	3978
		0.982[e]		1.598[e]		16.0[e]	1795[e]	3675[e]
$Zn_{3C}-O_{2C}$(J−I)	bared	0.954	120.6	1.710	93.8	4.7		
						5.6[e]		
	corner 2	0.955		1.711		43.4	1454	4106
		0.977[e]		1.664[e]		35.6[e]	1570[e]	3778
	reconst. step	0.951		1.767		26.0	1265	4103
		0.973[e]		1.702[e]		16.1[e]	1425[e]	3835[e]
$Zn_{2C}-O_{2C}$(F−G)	bared	0.952	121.1	1.617	124.0	87.2		
						65.0[e]		
	edge	0.951		1.602		41.7	1792	4113
		0.971[e]		1.589[e]		30.0[e]	1805[e]	3851[e]
$Zn_{2C}-O_{2C}$(D−E)	corner 1	0.951		1.644		64.8	1621	4092
						46.2[e]		
$Zn_{2C}-O_{2C}$(H−I)	corner 2	0.954		1.589		44.3	1850	4124
						31.4[e]		
exptl						∼30[c]	1485	3385
							−1753[d]	−3495[d]

[a] Positive value of ΔE means exothermicity. [b] The two letters in parentheses followed each clusters denote the active Zn and O ions, respectively, as those labeled in Figure 1. [c] Refs 7, 8. [d] Ref 10. [e] Calculated at MP2 level.

For the $Zn_{2C}-O_{3C}$(D−C) at corner site 1 or the $Zn_{3C}-O_{2C}$-(J−I) at corner site 2, embedding enhances the reactivity considerably, though this reactivity would have been overestimated owing to the neglect of surface reconstruction or relaxation. The reactivity of the former ion-pair is found to be slightly stronger than that of the latter. Inclusion of electron correlation results in about a 10 kcal/mol decrease of the calculated adsorption heat for both active sites. The adsorption heats calculated at the MP2 level are 38.5 and 35.1 kcal/mol for H_2 chemisorption on the $Zn_{2C}-O_{3C}$(D−C) and the $Zn_{3C}-O_{2C}$(J−I), respectively, which seem to be in reasonable agreement with experimental values.[7,8]

For the $Zn_{2C}-O_{2C}$ ion pairs located at an edge site, corner site 1, and corner site 2, their reactivities decrease considerably upon embedding with respect to the bare cluster. When comparing them with the $Zn_{2C}-O_{3C}$ and $Zn_{3C}-O_{2C}$ ion pairs, we found that after inclusion of the crystal potential, the difference between the reactivity of these defective ion-pairs becomes smaller, and they show similar reactivity to H_2 dissociation, i.e., 42−48 kcal/mol at the level of HF and 28−38 kcal/mol at the level of MP2, except that the $Zn_{2C}-O_{2C}$-(D−E) ion pair at corner site 1 has extraordinarily higher reactivity than any other sites.

C. Vibrational Frequencies. The recent FT-IR spectra of this chemisorption system were obtained by Boccuzzi et al.[10] on the ZnO powders. The assignment of absorption peaks can be summarized as follows: (i) the absorption bands between 3385 and 3495 cm^{-1} are ν(O−H)-derived; (ii) the absorption

peaks between 1485 and 1753 cm^{-1} are ν(Zn−H)-derived; (iii) the peaks located in the region of 640−950 cm^{-1} might be attributed to the δ(O−H), δ(Zn−H), γ(O−H), and some other bending vibrations. The evaluated vibrational frequencies of the Zn−H and O−H stretching modes by our SPC embedded cluster model calculations are given in Table 3. As shown by the Zn_5O_5 model, the chemisoprtion of H_2 on the $Zn_{3C}-O_{3C}$ ion pair, which is thermodynamically unfavorable, would result in a weak Zn−H bond. For the other the ion-pairs with low coordination numbers, the calculated Zn−H stretching frequencies range from 1454 to 1850 $cm^{-1}$and the computed O−H stretching frequencies are between 3978 and 4124 cm^{-1}, at the HF level. As compared with the results of HF, MP2 calculations generally shorten Zn−H bonds and lengthen O−H bonds. This leads to an increase of Zn−H stretching frequencies and a decrease of O−H stretching frequencies and brings the computed frequencies closer to those of the IR spectra. It is noted that the frequencies of X−H (X = Zn,O) show dependence on the coordination number of the respective X ion, i.e., the $Zn_{2C}-H$ and $O_{2C}-H$ stretching frequencies are much higher than those of the $Zn_{3C}-H$ and $O_{3C}-H$ vibrations, respectively.

5. The Effect of Surface Reconstruction on the Adsorption Properties. The $Zn_{2C}-O_{3C}$ or $Zn_{3C}-O_{2C}$ pairs at the corner of an ideal $(10\bar{1}0)$ surface can also be viewed as sites on polar (0001) and $(000\bar{1})$ surfaces. It is well-known, both experimentally and theoretically, that these polar surfaces must be reconstructed or relaxed so as to eliminate the dipole and to produce a stable surface, though theories disagreed with experiments on the details of reconstruction or relaxation.[13,26−31,38] LEED patterns of these polar surfaces indicated that these surfaces form steps.[26−29] Further analyses[25,29−31] of the LEED patterns of polar $(000\bar{1})$ surface showed the steps may be of a width of two double layer and a height of one unit cell in the $(10\bar{1}0)$ direction, as shown in Figure 3. In this subsection, we will consider the reactivity of the $Zn_{2C}-O_{3C}$ pair site located at a step of the $(000\bar{1})$ surface and the reactivity of $Zn_{3C}-O_{2C}$ pair site located at a step of the (0001) surface. These pair sites were modeled explicitly with a Zn_4O_4 cluster located at the edge of the middle step of a microcrystal having three steps on both the $(000\bar{1})$ and (0001) surfaces (see Figure 3). No relaxation of the surface atoms has been considered.

The calculated adsorption properties of these pair sites on the reconstructed surfaces are also presented in Table 3. H_2 is found to be chemisorbed heterolytically on these pair sites with adsorption heats around 20 kcal/mol. Hence reconstruction does reduce the reactivities of the $Zn_{2c}-O_{3C}$ and the $Zn_{3C}-O_{2C}$ pair sites toward H_2, as compared with the reactivity of the corresponding pair site on the ideal surface. On the reconstructed step sites, MP2 O−H stretching frequencies on O_{3c} and O_{2c} are 3675 and 3835 cm^{-1}; while MP2 Zn−H stretching frequencies on Zn_{3c} and Zn_{2c} are 1425 and 1795 cm^{-1}.These values can be favorably compared with the experimental data of 3385−3495 cm^{-1} for ν(O−H) and 1485−1753 cm^{-1} for ν(Zn−H). Again, we find that the frequencies of X−H (X = Zn,O) are site-dependent with $Zn_{2C}-H$ and $O_{2C}-H$ stretching frequencies being higher than those of the $Zn_{3C}-H$ and $O_{3C}-H$ vibrations, respectively.

6. The Influence of Different Embedding Schemes on the Simulation Results

We have shown that the heterolytic chemisorption of H_2 at the $Zn_{3C}-O_{3C}$ pair site (site A−B in Figure 1) on the ZnO-$(10\bar{1}0)$ surface is endothermic with the calculated reaction heats of 22.9 kcal/mol at HF level and 23.6 kcal/mol at the level of MP2. It is noteworthy that the microcrystal shown in Figure 1 is terminated by a polar Zn(0001) surface on the left side and a polar $O(000\bar{1})$ surface on the right side. Clearly, such embedding scheme results in a net dipole moment along the *x*-axis, which may add an unrealistic electrostatic contribution to the adsorption on site A−B. Furthermore, increasing the microcrystal by one layer of atoms on each side will alter the direction of the dipole along the *x*-axis. This gives rise to two interesting questions: (i) in which way does the alternating dipole influence the simulation results? (ii) how can we reach converged simulation results by choosing suitable embedding scheme?

TABLE 4: Calculated Heats of $H_2/Zn_{3C}-O_{3C}$(A−B) with Different Embedding Schemes

	ΔE^a(kcal/mol)	
	HF	MP2
Scheme 1	−22.9	−23.6
Scheme 2	49.8	37.4
Scheme 3	−22.6	−23.6
Scheme 4	−21.4	−22.9

[a] Positive value of ΔE means exothermicity.

To answer these questions, we have investigated the effect of different embedding schemes, shown in Figure 4, on the calculated adsorption properties of site A−B. Embedding scheme 1 of Figure 4 is identical to that of Figure 1. Scheme 2 was obtained by adding one layer of atoms to each side of the microcrystal of Scheme 1. In Scheme 3, a close double layer was added on both sides of the microcrystal of Scheme 1. In Scheme 4, only one close double layer on the right side was added to the microcrystal of Scheme 1. Judging by the structures of these four microcrystals, it is clear that Scheme 2 should give the largest net dipole moment along the *x*-axis; while the net dipole moments (along the *x*-axis) of other schemes should be similar. Accordingly, embedding Scheme 2 would lead to the worst simulation results. Table 4 gives the reaction heats of the heterolytic chemisorption of H_2 on site A−B from different embedding schemes. With embedding Scheme 2, the reaction is predicted to be exothermic, in contradiction with the experimental observation. Embedding schemes 1, 3, and 4 give converged calculation results, which qualitatively agree with the experimental observation. In the modeling of TiO_2(110) surface, we have seen that keeping the symmetry of PCC is very important for eliminating the unrealistic dipole moment.[16] In the case of ZnO, it seems that terminating the embedding microcrystal by a close double layer and enlarging the embedding microcrystal by adding double layers will give converged simulation results.

7. Concluding Remarks

Heterolytic adsorption of H_2 on ZnO$(10\bar{1}0)$ surface has been investigated by means of an ab initio embedded cluster method. The spherical charges, rather than the simple point charges, have been employed to embed the cut-out clusters, and the values of the spherical charges are maintained to be self-consistent with those of the embedding cluster. Several possible adsorption sites have been considered. The effect of the shape of PCC and the influence of the surface reconstruction on the calculated adsorption properties have been investigated. Our main calculation results can be summarized as follows:

(a) The calculated electronic properties of the $Zn_{3c}-O_{3c}$ perfect ion pair are similar to those of bulk solid; while those of the defective ion pairs differ considerably. Ions at differently coordinated and exposed sites at the surface have a variable

ionicity, different amounts of atomic orbital characters in the frontier orbitals, and a different reactivity.

(b) The heterolytic adsorption of H_2 on ZnO($10\bar{1}0$) surface is site-dependent, taking place only on those Zn−O ion pairs with low coordination numbers, such as $Zn_{2c}-O_{3c}$, $Zn_{3c}-O_{2c}$, and $Zn_{2c}-O_{2c}$, rather than on the perfect ion pair, $Zn_{3c}-O_{3c}$. Reconstruction tends to reduce the reactivity of the defective ion pairs.

(c) The effect of the crystal potential is significant. It is important to keep the symmetry of PC array so as to eliminate the unrealistic dipole moment. The results from the bared cluster model calculations could only be regarded as qualitative. The calculated adsorption heats with the bare Zn_4O_4 cluster models are either too low (3.0−8.0 kcal/mol) or too high (65.0−87.2 kcal/mol) as compared with the experimental value (∼30.0 kcal/mol), while the calculated adsorption heats with the SPC embedded cluster models are in good agreement with the experimental values.

(d) The predicted Zn−H and O−H stretching frequencies are in reasonable accordance with those of the IR spectra. The frequencies of X−H (X = Zn,O) show dependence on the coordination number of the respective X ion, i.e., the $Zn_{2C}-H$ and $O_{2C}-H$ stretching frequencies are much higher than those of the $Zn_{3C}-H$ and $O_{3C}-H$ vibrations, respectively. It is also found that the lower coordination number the X ion possesses, the shorter the H−X bond length is.

Acknowledgment. We thank the referee for his critical review. This work is supported by the National Nature Science Foundation of China, the doctoral project foundation of the State Education Commission of China, the Fok Ying Tung Education Foundation, and the Japan Society for Promotion of Science.

References and Notes

(1) Taylor, H. S.; Strother, C. O. *J. Am. Chem. Soc.* **1934**, *56*, 589.
(2) Eischens, R. P.; Pliskin, W. A.; Low, M. J. D. *J. Catal.* **1962**, *1*, 180.
(3) Dent, A. L.; Kokes, R. J. *J. Phys. Chem.* **1969**, *73*, 3781.
(4) Baranski, A.; Cvetanovic, R. J. *J. Phys. Chem.* **1971**, *75*, 208.
(5) Kokes, R. J.; Dent, A. L.; Chang, C. C.; Dixon, L. T. *J. Am. Chem. Soc.* **1972**, *94*, 4429.
(6) Kokes, R. J. *Acc. Chem. Res.* **1973**, *6*, 222, and references therein.
(7) Bowker, M.; Houghton, H.; Waugh, K. C. *J. Chem. Soc., Farady Trans. 1* **1981**, *77*, 3023.
(8) Waugh, K. C. *Catalysis Today* **1992**, *15*, 51.
(9) Griffin, G. L.; Yates, J. T. *J. Catal.* **1982**, *73*, 396.
(10) Ghiotti, G.; Chiorino, A.; Boccuzzi, F. *Surf. Sci.* **1993**, *287*, 228.
(11) Anderson, A. B.; Nichols, J. A. *J. Am. Chem. Soc.* **1986**, *108*, 4742.
(12) Nakatsuji, H.; Fukunishi, Y. *J. Int. Quantum Chem.* **1992**, *42*, 1101.
(13) Nyberg, M.; Nygren, M. A.; Pettersson, L. G. M.; Gay, D. H.; Rohl, A. L. *J. Phys. Chem.* **1996**, *100*, 9054.
(14) Martins, J. B. L.; Taft, C. A.; Longo, E.; Andres J. *J. Mol. Struct.−Theochem.* **1997**, *397*, 147.
(15) Martins, J. B. L.; Longo, E.; Taft, C. A.; Andres J. *J. Mol. Struct.−Theochem.* **1997**, *398*, 457.
(16) Xu, X.; Nakatsuji, H.; Ehara, M.; Lü, X.; Wang, N. Q.; Zhang, Q. E. *The Fourth Japan-China Theoretical Symposium on Theoretical Chemistry*, p 52, Kyoto, Japan, 1996, 9.
(17) Lü, X.; Xu, X.; Wang, N.; Zhang, Q.; Ehara, M.; Nakatsuji, H. *Chem. Phys. Lett.* **1998**, *291*, 445.
(18) Lü, X.; Xu, X.; Wang, N.; Zhang, Q. *J. Chem. Chin. University* **1998**, *19*, 783.
(19) Kunz, A. B. *Int. J. Quantum Chem. Symp.* **1990**, *24*, 607.
(20) Sauer, J. *Chem. Rev.* **1989**, *89*, 199.
(21) Barandiarán, Z.; Seijo, L. *J. Chem. Phys.* **1988**, *89*, 5739.
(22) Xu, X.; Lü, X.; Wang, N.; Zhang, Q. *Chem. Phys. Lett.* **1995**, *235*, 541.
(23) Xu, X.; Nakatsuji, H.; Ehara, M.; Lü, X.; Wang, N. Q.; Zhang, Q. E. *Science in China* **1998**, *41*, 113.
(24) Xu, X.; Nakatsuji, H.; Ehara, M.; Lü, X.; Wang, N. Q.; Zhang, Q. E. *Chem. Phys. Lett.* **1998**, *292*, 282.
(25) Abrahams, S. C.; Bernstein, J. L. *Acta Crystallogr.* **1989**, *B25*, 1233.
(26) Chang, S.-C.; Mark, P. *Surf. Sci.* **1974**, *46*, 293.
(27) Duke, C. B.; Lubinsky, A. R. *Surf. Sci.* **1975**, *50*, 605.
(28) van Hove, H.; Leysen, R. *Phys. Status Solidi A*, **1972**, *9*, 361.
(29) Møller, P. J.; Komolov, S. A.; Lazneva, E. F. *Surf. Sci.* **1994**, *318*, 379.
(30) Henzler, M. *Surf. Sci.* **1973**, *36*, 109.
(31) Henrich, V. E.; Zeiger, H. J.; Solomon, E. I.; Gay, R. R. *Surf. Sci.* **1978**, *74*, 682.
(32) Hay, P. J.; Wadt, W. R. *J. Chem. Phys.* **1985**, *82*, 270.
(33) Dunning, T. H., Jr. *J. Chem. Phys.* **1970**, *53*, 2823.
(34) Stevens, W. J.; Basch H.; Jrauss, M. *J. Chem. Phys.* **1984**, *81*, 6026.
(35) Frisch, M. J.; Trucks, G. W.; Schlegel, H. B.; Gill, P. M. W.; Johnson, B. G.; Robb, M. A.; Cheeseman, J. R.; Keith, T.; Petersson, G. A.; Montgomery, J. A.; Raghavachari, K.; Al-Laham, M. A.; Zakrzewski, V. G.; Ortiz, J. V.; Foresman, J. B.; Peng, C. Y.; Ayala, P. Y.; Chen, W.; Wong, M. W.; Andres, J. L.; Replogle, E. S.; Gomperts, R.; Martin, R. L.; Fox, D. J.; Binkley, J. S.; Defrees, D. J.; Baker, J.; Stewart, J. P.; Head-Gordon, M.; Gonzalez, C.; Pople, J. A. *Gaussian 94*; Gaussian, Inc.: Pittsburgh, PA, 1995.
(36) Sawabe, K.; Koga, N.; Morokuma, K. *J. Chem. Phys.* **1992**, *97*, 6871.
(37) Kobayashi, H.; Salahub, D. R.; Ito, T. *J. Phys. Chem.* **1994**, *98*, 5487.
(38) Nosker, R. W.; Mark, P.; Levine, J. D. *Surf. Sci.*, **1970**, *19*, 291.